Experimental investigation of the effect of dynamic melting in a cylindrical shell-and-tube heat exchanger using water as PCM

Jaume Gasia[1], N.H. Steven Tay[2,3,*], Martin Belusko[2], Luisa F. Cabeza[1], Frank Bruno[2]

[1]GREA Innovació Concurrent, Universitat de Lleida, Edifici CREA, Pere de Cabrera s/n, 25001, Lleida, Spain

[2]Barbara Hardy Institute, University of South Australia, Mawson Lakes Boulevard, Mawson Lakes, South Australia 5095, Australia

[3]School of Mechanical and Systems Engineering, Newcastle University International Singapore, 172A Ang Mo Kio Avenue 8, #05-01, SIT Building@Nanyang Polytechnic, Singapore 567739, Singapore

*Corresponding author: Tel: +65 6908 6682. Email: steven.tay@newcastle.ac.uk

Abstract

In the present paper, an experimental study is carried out to evaluate the effect of the dynamic melting concept in a cylindrical shell-and-tube heat exchanger using water as the phase change material (PCM) and a potassium formate/water solution as the heat transfer fluid (HTF). The dynamic melting concept is a new heat transfer enhancement technique which consists of recirculating the liquid PCM during the melting process with a pump and thus increasing the overall heat transfer coefficient as a result of the dominance of the forced convection. The HTF flow rate was kept constant at 1 *l*/min and four different PCM flow rates of 0, 0.5, 1 and 2 *l*/min were tested. Results from the experimental analysis showed enhancements up to 65.3% on the melting period, up to 56.4% on the effectiveness, and 66% on the heat transfer rates when the PCM flow rate was twice the HTF flow rate. From these experiments it can be concluded that dynamic melting is an effective technique for enhancing heat transfer during melting of PCM.

Keywords: Thermal energy storage; Phase change material; Dynamic melting; Heat transfer enhancement; effectiveness.

Nomenclature

Dimensional variables

A	Area (m^2)
cp	Specific heat (J/kg·K)
E	Energy (J)
$\dot{m}$	Mass flow rate (kg/s)
$\dot{Q}$	Heat transfer rate (W)
r	Radial dimension of the HTF tube (m)
T	Temperature (ºC)
$\dot{V}$	Volumetric flow rate (m^3/s)

Greek symbols

α	Convection coefficient ($W/m^2 \cdot K$)
δ	Error of the energy balance (-)
ε	Local effectiveness (-)
η	Efficiency (-)
λ	Thermal conductivity (W/m·K)
ρ	Density (kg/m^3)

Subscripts

1	HTF tube
2	Inner face of the heat exchanger
3	Outer face of the heat exchanger
4	Outer face of the insulation
amb	Ambient
c	Cross sectional
in	Inlet of the heat exchanger
ins	Insulation
HEX	Heat exchanger
$HG.loop$	Heat gains as a result of the external recirculation of the liquid PCM
$HG.BC$	Heat gains as a result of the boundary conditions
HTF	Heat transfer fluid
L	Losses
m	Melting
$Near.Tube.ave$	Average near the HTF pipe
out	Outlet of the heat exchanger

p	Pump
PC	Phase change
PCM	Phase change material
ps	Power station
theor	Theoretical

1 Introduction

It is well understood that the implementation of energy storage technologies is an effective method to help to correct the mismatch between the energy demand and supply. Among the different thermal energy storage technologies, latent heat thermal energy storage (LHTES) systems, have gained relevance during the last decades because of their high energy storage densities and almost isothermal operating conditions [1].

In LHTES systems, the process of energy storage involves absorbing (charging) and releasing (discharging) thermal energy. During these processes, the phase change material (PCM) stores and releases thermal energy when changing from a solid to a liquid. In low temperature storage applications (cold storage), charging involves freezing while discharging involves melting. During the charging process, the PCM solid front moves away from the heat transfer surface and the thickness of the PCM solid layer increases. This makes conduction the dominant heat transfer mechanism. During the discharge process, the PCM starts melting around the heat transfer surface. The melting front moves away from the heat transfer surface and the thickness of the PCM liquid layer increases. Thus, the conduction becomes the heat transfer mechanism. In both cases the thermal resistance increases, reducing the effectiveness of heat transfer.

The low thermal conductivity coefficients of currently-available cost-effective PCMs cause the thermal resistance to be high, so it reduces the heat transfer during the charging processes [2]. To overcome this drawback and to improve the thermal performance of the thermal energy storage system, heat transfer enhancement techniques are required. These techniques consist of adding extended surfaces, such as fins [3,4] and heat pipes [5,6], and combining the PCM with highly conductive materials, such as carbon-based elements [2,7], metallic particles elements [8] and nanoparticles [9]. However, adding external elements to improve the thermal conductivity causes a decrease in the energy storage capacity, a decrease in the compactness factor, which is the ratio that takes into account the volume of PCM per volume of LHTES unit, and an increase of the final cost of the system.

Researchers have recently investigated improving the thermal performance during the melting process. The enhancement is based on moving the PCM while undergoing phase change with an external mechanical force [10-13]. This causes forced convection to become the dominant heat transfer mechanism and therefore helps to increase the overall heat transfer coefficient. Three main advantages are associated with this heat transfer enhancement technique. First, a higher heat transfer rate can be maintained for a longer period during phase change. Second, the continuous movement of PCM may avoid phase segregation. Third, the compactness factor of the storage tank is kept constant since no external elements are introduced inside the LHTES unit. The main disadvantages of this enhancement technique are the increase of the electrical energy consumption required by actively pumping the PCM and the increase of the heat exchanged within the surroundings (heat losses or heat gains, depending on the temperature range).

In recent times, only three studies have investigated the benefits of actively moving the PCM to improve the heat transfer: screw heat exchanger, PCM flux, and dynamic melting. Zipf et al. [10] presented a study based on the main principles of the screw heat exchanger design and construction. This concept consists of a heat exchanger which has an internally helicoidally heat transfer surface that is continuously moving. It transports the PCM during both melting and solidification processes, from a PCM storage tank, which is located at one end of the heat exchanger and where the PCM is in one state, to another PCM storage tank, which is located at the other end of the heat exchanger and where the PCM is stored in the other state. Pointner et al. [11] presented the PCM flux concept, which consists of a transportation line that moves macro-encapsulated PCM blocks parallel to a heat transfer surface. The PCM is mechanically separated from the heat transfer surface by an intermediate fluid layer to ensure the thermal conduction. Finally, the dynamic melting concept was experimentally and numerically investigated by Tay et al. [12,13]. This concept consists of externally recirculating the liquid PCM with a pump during the melting process. In the first work, Tay et al. [12] designed and constructed a tube-in-tank LHTES system with two pre-melt tubes which created the pre-melt paths to allow dynamic melting. Results showed an improvement of up to 89 % in the average effectiveness and up to 30 % decrease in the melting period. In order to study the benefits of dynamic melting more directly, Tay et al. [13] numerically studied the effect of both heat transfer fluid (HTF) and PCM mass flow rates and direction (parallel and counter-flow) for the dynamic melting enhancement technique in a shell-and-tube heat exchanger. Results showed that the counter-flow direction delivered lower phase change periods than the parallel-flow direction. It was also found that when the flow rates of the PCM were equal or higher than the HTF, better results were obtained in terms of effectiveness and phase change periods.

The aim of the research work presented in this paper is to experimentally investigate the effect of dynamic melting in a shell-and-tube heat exchanger consistent with the CFD study completed by Tay et al. [13], using water as the PCM. This investigation will contribute to the knowledge of these techniques by experimentally verifying the conditions by which dynamic melting can dramatically increase heat transfer.

2 Experimental study

2.1 Experimental set-up

A schematic view of the experimental set-up is shown in Fig. 1. It is composed of the following components: (1) a shell-and-tube heat exchanger; (2) a cold HTF tank, which stored and cooled 400 *l* of HTF with a refrigeration unit; (3) a hot HTF tank containing 25 *l* of HTF, which was stored and maintained at the desired discharging temperature with an electrical heater and a temperature controller; (4) two Keg King MK II magnetic drive pumps, which recirculated the HTF and the liquid PCM; (5) two three-way valves, which were used to change the direction of the HTF so as to switch between charging and discharging processes; (6) two pin valves, which were used to adjust the flow rates of the HTF and the PCM; and finally, (7) a data acquisition unit connected to a personal computer (PC) for data analysis. All the components which were likely to exchange heat with the surroundings were insulated with 95 mm of expanded polystyrene.

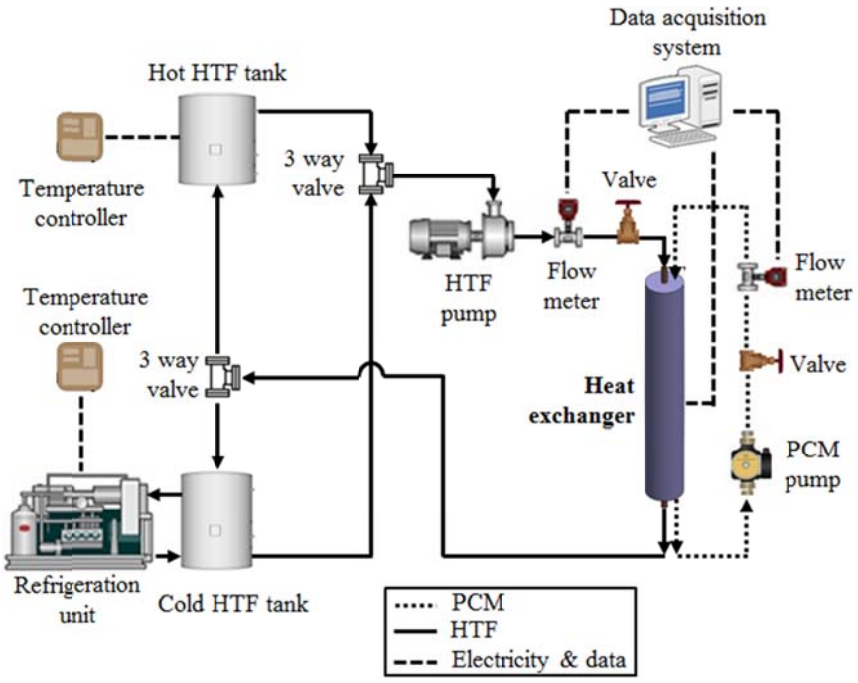

Fig. 1. Schematic view of the experimental set-up used to perform the present work.

The heat exchanger is based on the shell-and-tube concept. It composed of two concentric tubes, with the HTF flowing vertically through the inner tube and with the PCM placed in the annulus region between the two tubes (Fig. 2). The inner tube is made of stainless steel and has an outer diameter of 25.4 mm. The outer tube, or shell, is made of clear polycarbonate, which allows visual inspection of the heat exchanger. It has a length of 1006 mm, with inner and outer diameters of 94 mm and 100.6 mm, respectively. The HTF used was a potassium formate and water solution. It has an operating temperature range of -50 ºC to 218 ºC. At −10 °C, the viscosity of the HTF is 5.99 mPa·s, the thermal conductivity is 0.475 W/m·K, the specific heat is 2.64 kJ/kg·K, and the density is 1356 kg/m^3. At 10 °C, the viscosity of the HTF is 3.80 mPa·s, the thermal conductivity is 0.495 W/m·K, the specific heat is 2.68 kJ/kg·K, and the density is 1345 kg/m^3. Water was used as the PCM to eliminate the errors associated with latent energy measurement. It was placed in the annulus space between the metallic tube and the plastic shell, to a height of 926 mm, leaving 50 mm height of air for volumetric expansion. Different temperature sensors, as shown in Fig. 2, determined the thermal behaviour of the system during the experimentation. Five four-wire resistance temperature detectors (RTDs) with an error of ±0.1 °C were placed inside the PCM at axial distances of 115 mm, 246 mm, 486 mm, 726 mm, and 861 mm from the bottom of the heat exchanger and at radial distances of 17.7 mm and 40 mm. Four more RTDs were placed at the inlet and outlet of both the HTF and the PCM recirculation loop to obtain accurate temperature measurements of the HTF and the liquid PCM during the dynamic melting process. Two rotary piston flow meters with an error of ±2% were used to measure both the HTF and the liquid PCM flow rates. All RTDs and flow meters were connected to a data acquisition system. Commercial software was used to acquire and record the data at time intervals of 5 s in a database format on the PC for further processing. The sensors and flow meters were calibrated with the data acquisition system so that the errors were minimised.

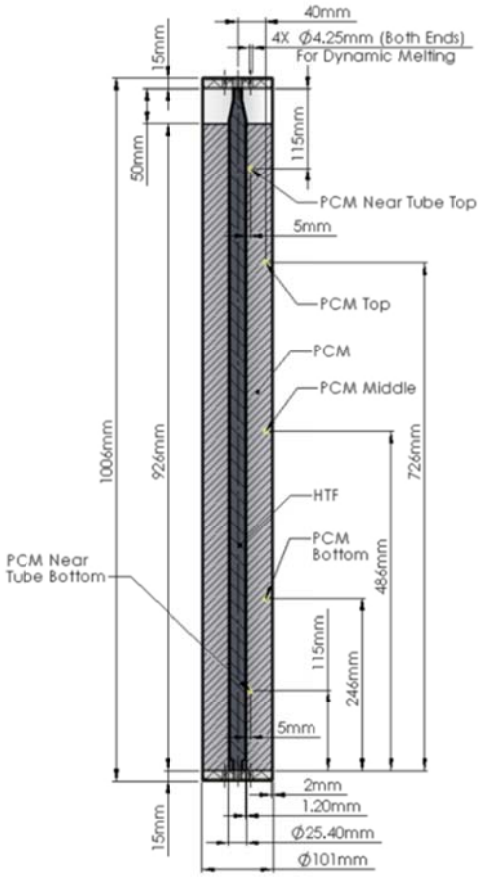

Fig. 2. Schematic view of the shell-and-tube heat exchanger. Dimensions and location of the temperature sensors.

2.2 Methodology

2.2.1 Experimental procedure

The experiments consisted of different charging (freezing) and discharging (melting) processes at a temperature range between -7.5 ºC and 10 ºC. The HTF flow rate was set at a constant value of 1 *l*/min for all the experiments and the PCM flow rates were modified to 0.5, 1 and 2 *l*/min. A baseline test was also conducted without any PCM flow.

For each test the PCM was frozen to achieve the same initial conditions. The HTF was set at the temperature of -7.5 ºC and it was circulated through the inner tube from the top to the bottom, until all the temperature sensors inside the PCM were recording the same temperature of -4 ±1 ºC. Subsequently, the discharging processes were performed. Three different repetitions for each test were carried out to ensure repeatability. They were conducted by circulating the HTF at a temperature of 10 ºC through the inner tube from the top to the bottom until the PCM reached the HTF temperature. As for the discharging processes with dynamic melting, the start

of the tests was the same as the baseline test. Dynamic melting processes were activated when the PCM temperature close to HTF tube (*PCM Near Tube Top* and *PCM Near Tube Bottom*) reached 5 ±0.5 ºC. It was experimentally proven that this temperature was the threshold for a liquid path to be created. The start of the dynamic melting process represents a variable in the impact of such a technique on the results overall effectiveness. The recirculation of the liquid PCM was then conducted by pumping it from the bottom of the heat exchanger and returning it to the top, such that the PCM flow was in parallel to the HTF.

2.2.2 Calculation procedure

The energy absorbed by the PCM during the discharging process is equal to the summation of the energy which is actually recovered by the HTF (E_{HTF}), the heat gains because of the boundary conditions ($E_{HG.BC}$), and the heat gains due to external recirculation of the liquid PCM ($E_{HG.loop}$). This parameter is defined in Eq. 1:

$$E_{PCM} = E_{HTF} + E_{HG.BC} + E_{HG.loop} = \int^{t_{PC}} (\dot{Q}_{HTF} + \dot{Q}_{HG.BC} + \dot{Q}_{HG.loop}) \cdot dt \quad (1)$$

The HTF heat transfer rate ($\dot{Q}_{HTF}$) is calculated using Eq. 2:

$$\dot{Q}_{HTF} = \dot{m}_{HTF} \cdot cp_{HTF} \cdot (T_{HTF.in} - T_{HTF.out}) \quad (2)$$

where $\dot{m}_{HTF}$ is the mass flow rate of the HTF, cp_{HTF} is the specific heat of the HTF, and $(T_{HTF.in} - T_{HTF.out})$ is the temperature difference of the HTF between the inlet and the outlet of the heat exchanger.

The heat transfer rate of the heat gains because of the boundary conditions ($\dot{Q}_{HG.BC}$) is defined in Eq. 3:

$$\dot{Q}_{HG.BC} = \frac{T_{PCM.Near.Tube.ave} - T_{amb}}{\frac{\ln(r_2/r_1)}{2 \cdot \pi \cdot \lambda_{PCM}} + \frac{\ln(r_3/r_2)}{2 \cdot \pi \cdot \lambda_{HEX}} + \frac{\ln(r_4/r_3)}{2 \cdot \pi \cdot \lambda_{ins}} + \frac{1}{2 \cdot \pi \cdot r_4 \cdot \alpha_{air}}} \quad (3)$$

where, $T_{PCM.Near.Tube.ave}$ is the average temperature of the PCM near the HTF tube, T_{amb} is the ambient temperature, r_1, r_2, r_3, and r_4 are the radial dimension of the HTF tube, inner face of the shell, outer face of the shell, and outer face of the insulation, respectively. λ_{PCM}, λ_{HEX}, and λ_{ins} are the thermal conductivities of the PCM, polycarbonate and insulation, respectively, and

α_{air} is the air convection coefficient. In order to facilitate the calculation of this parameter, it was assumed that it consists of a one dimensional process, conduction is the only heat transfer mechanism in the PCM, and with insulation the convection has a negligible impact.

Finally, the heat transfer rate of the heat gains due to external recirculation of the liquid PCM are mainly caused by two factors. First, the heat introduced by the recirculation pump as a result of its internal mechanical losses, and second, the heat absorbed along the PCM recirculation loop through the insulated piping. This parameter is calculated as shown in Eq. 4:

$$\dot{Q}_{HG.loop} = \dot{m}_{PCM} \cdot cp_{PCM} \cdot (T_{PCM.in} - T_{PCM.out}) \quad (4)$$

where $\dot{m}_{PCM}$ is the mass flow rate of the PCM liquid fraction, cp_{PCM} is the specific heat of the liquid PCM, and $(T_{PCM.in} - T_{PCM.out})$ is the temperature difference of the liquid PCM between the inlet and the outlet of the heat exchanger.

The heat introduced by the recirculation pump (P_L) determines the influence of the pump in the PCM heating rate. This value is calculated as shown in Eq. 5:

$$P_L = \frac{\Delta P \cdot \dot{V}_{PCM}}{\eta_p \cdot \eta_{ps}} \quad (5)$$

where ΔP is the pressure drop of the PCM liquid fraction in the PCM recirculation loop, evaluated with the Darcy-Weisbach equation (Eq. 6). $\dot{V}_{PCM}$ is the volumetric flow rate of the liquid PCM during the dynamic melting. Pump efficiency (η_p) and power station efficiency (η_{ps}) were fixed at 0.5 and 0.3, respectively.

$$\Delta P = f \cdot \left(\frac{L}{d}\right) \cdot \left(\frac{\dot{m}_{PCM}^2}{2 \cdot \rho_{PCM} \cdot A_c^2}\right) \quad (6)$$

where f is the friction factor, L is the length of the PCM recirculation loop, d is the inner tube diameter, Ac is the cross sectional area of the annulus between the HTF tube and the shell, ṁ the mass flow rate of the liquid PCM in the PCM recirculation loop and ρ is the density of the liquid PCM. The entrance and exit losses are ignored as these are negligible.

Local effectiveness, as described in Eq. 7, is the ratio of the actual heat transfer and the theoretical maximum heat transfer that can be discharged at any point in time over the phase

change period [14]. Therefore, the maximum values of effectiveness are obtained when the HTF exits at temperatures close to the PCM phase change temperature.

$$\varepsilon = \frac{\dot{Q}_{experiment}}{\dot{Q}_{theoric}} = \frac{T_{HTF.in} - T_{HTF.out}}{T_{HTF.in} - T_{PCM.m}} \quad (7)$$

In order to validate the results, the error from the energy balance is calculated as shown in Eq. 8:

$$\delta = \frac{E_{PCM.PC} - E_{theor.PC}}{E_{theor.PC}} \quad (8)$$

where $E_{PCM.PC}$ is the energy absorbed during the phase change process from the energy balance shown in Eq.1, and $E_{theor.PC}$ is the theoretical energy absorbed. This last parameter is calculated multiplying the PCM mass and the PCM heat of fusion. Sensible energy is ignored since it only represents 13.5 % of the energy stored in the PCM

3 Results and discussion

Fig. 3 to Fig. 6 present the temperature evolution of the PCM and the inlets and outlets of the HTF and PCM during the discharging process for four different PCM flow rates. The PCM temperature evolution along the discharging process allows the influence of the dynamic melting on the phase change process to be studied.

Fig. 3 shows the temperature distribution for the baseline test with the HTF flow rate of 1 *l*/min and the PCM flow rate of 0 *l*/min. In this figure, three different states of the test can be clearly observed. The first one is the solid sensible region, where the top, middle and bottom PCM temperatures showed a nearly homogeneous increase, from the initial discharging conditions to the phase change temperature. This behaviour shows that conduction is the main heat transfer mechanism and gravity has no effect on the solid PCM. Once the PCM reached the phase change temperature (0.11 h), it moved to the latent heat transfer region. After 0.3 h, a melted path started to be formed around the HTF tube since the PCM temperature sensors located near the outer surface of the HTF tube (*PCM Near Tube Top* and *PCM Near Tube Bottom*) showed that the temperatures were higher than zero. The separation of ice from different surfaces of the inner and outer tubes played an important role on the PCM temperature distribution. This was consistent with López-Navarro et al. [15]. While the *PCM Near Tube Bottom* thermocouple showed a gradual increase during the melting process, the *PCM Near Tube Top* showed different peaks along the melting process. Since water has a lower density in the solid state than

in liquid state (unlike most of the other PCMs), once the ice was detached from the surfaces of the heat exchanger, it floated, and remained around the upper PCM temperature sensors. As a result, the upper region of the PCM was kept in the latent region for a longer time than the lower region. This result is unlikely to have occurred without the impact of buoyancy. Since the HTF flows from top to bottom, consistent with Tay et al. [13], the upper section should complete melting before the lower sections. Finally, after 12.4 h it can be considered that the PCM entered the liquid sensible region, and therefore the melting process lasted 12.3 h. In the liquid sensible region, the PCM temperature behaviour followed a different pattern than the one observed in the latent region, showing a temperature stratification mainly influenced by the HTF flow arrangement and the effect of natural convection. When the PCM was in a liquid state, the heat transfer was mainly conducted by natural convection, which created an internal recirculation due to the buoyancy forces. These forces are induced by the density gradients as a result of the temperature differences [16]. Notice that during the liquid sensible region, there was a sharp decrease in the *PCM Near Tube Top* temperature sensor. This result can be attributed to a small piece of ice attached at the top layers of the heat exchanger that was broken up towards the end of the process and floated on top of the liquid PCM.

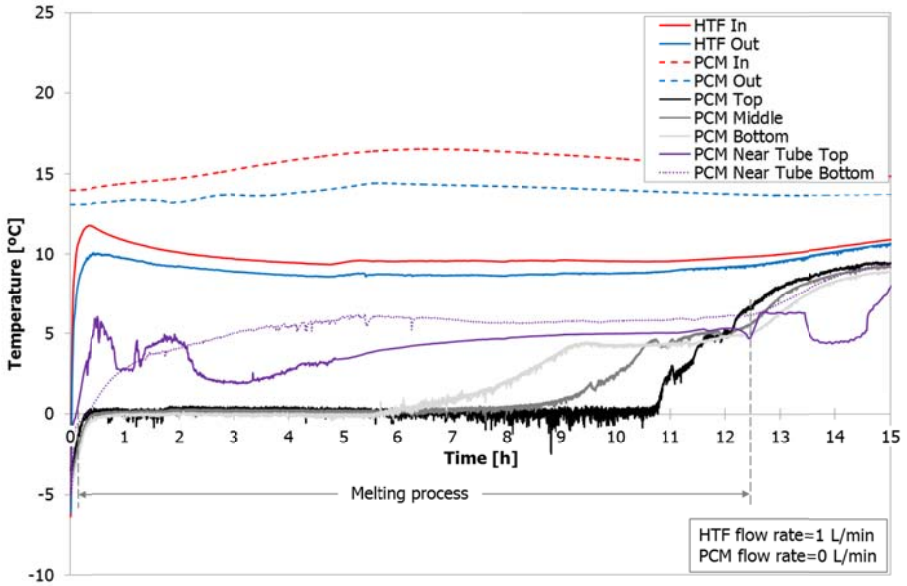

Fig. 3. Temperature evolution of the heat transfer fluid (HTF) and the phase change material (PCM) of the baseline test. Experimentation set at an average HTF flow rate of 1 *l*/min and a PCM flow rate of 0 *l*/min.

Fig. 4 to Fig. 6 show the temperature distribution for an HTF flow rate of 1 *l*/min and PCM flow rates of 0.5, 1 and 2 *l*/min, respectively. In all these experiments, the behaviour of the PCM before starting the dynamic melting process was similar to the baseline test, confirming that the experimental results are directly comparable. The phase change of all three experiments started

at 0.12 ±0.02 h after the beginning of the melting process, and the dynamic melting processes started 0.7 ±0.05 h after the start of the discharging processes. Despite the variation in the start of dynamic melting processes, it has a small effect on the results of dynamic melting, especially on the overall effectiveness, as it is observed in the following sections. When the PCM recirculation pump was switched on, a sharp variation in the temperature of recirculated PCM (*PCM in* and *PCM out*) was observed. Before starting the dynamic melting processes, the PCM located inside the PCM recirculation loop was at a temperature close to the ambient one as a result of being located outside the heat exchanger zone, although insulated from the surroundings. Immediately after starting the dynamic melting process, these temperatures decreased as the PCM was recirculated. The sensors *PCM Near Tube Top* and *PCM Near Tube Bottom* also showed a sharp variation for analogous reasoning. Once the dynamic melting processes started, the inlet and outlet temperatures of the HTF remained relatively constant throughout the phase change period for 0.5 *l*/min and decreased at higher PCM flow rates. This decrease is indicative of the improved heat transfer to the HTF, as the PCM could absorb more energy than that applied to the HTF from the heat source. It was observed that, when the PCM flow rate was equal or higher than the HTF flow rate, the temperature differences between the inlet and outlet HTF increased due to the decreasing outlet HTF temperature, as predicted by Tay et al. [13]. The reason is because for PCM flow rates lower than HTF flow rates, the heat gains associated with the recirculation outside the heat exchanger of the liquid PCM has a higher influence in heat transfer than the enhancement obtained as a result of the forced convection. Hence, the enhancement obtained as a consequence of the increase in the overall heat transfer coefficient was compensated or even overcome for the PCM temperature increase as a result of the heat gains.

The PCM temperature profiles during the dynamic melting processes in the latent region varied significantly depending on the PCM flow rates. When the PCM flow rate was equal or lower than the HTF flow rate, the phase change within the heat exchanger followed the following pattern: *PCM Top>PCM Middle>PCM Bottom*, consistent with the baseline case. When the PCM flow rate was higher than the HTF flow rate, the phase change within the heat exchanger followed the following pattern: *PCM Middle>PCM Top>PCM Bottom*. During melting, buoyancy in the PCM maintained the warm liquid near the top and therefore this section melted first. With a high level of forced flow, this buoyancy was overpowered and therefore the PCM liquid was further mixed, changing which section melted first. At the end of the melting process, remaining ice located at the bottom region of the heat exchanger was detached from the surface of the heat exchanger and raised to the top of the PCM column reducing top temperatures.

From this study, it can be observed that the phase change duration was reduced as the PCM flow rate increased since the overall heat transfer coefficient was increased. Moreover, the temperature difference in the PCM recirculation loop shows that heat was being transferred to the PCM as it was pumped and this heat did contribute to the melting process, and therefore influenced the decreasing of the melting time. Hence, as a result of recirculating the liquid PCM, the melting processes with a flow rate of 0.5, 1 and 2 *l*/min were completed after 6.61, 6.55 and 4.26 h, respectively, representing the melting processes to be 47.4%, 47.8% and 65.3% faster than the baseline test.

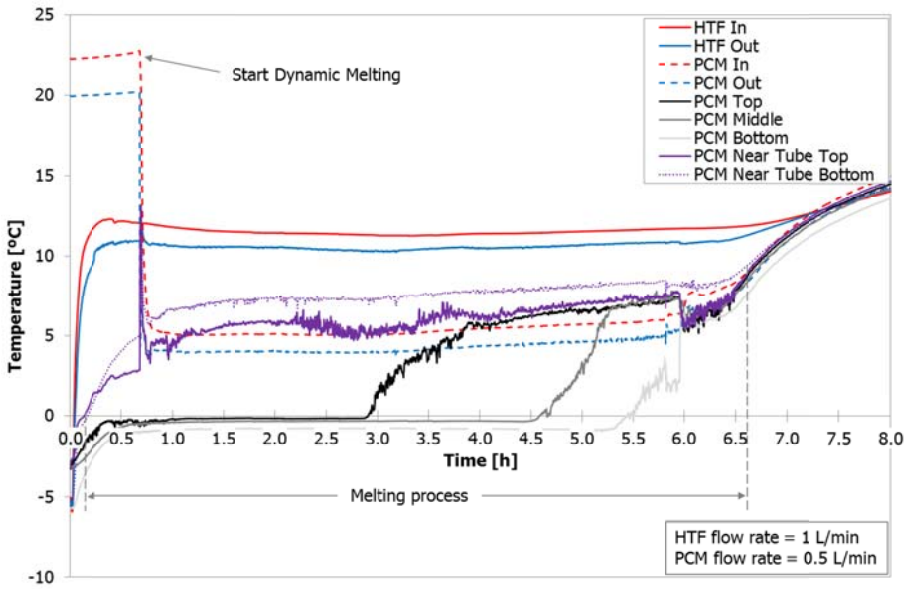

Fig. 4. Temperature evolution of the HTF and the PCM in a discharging process with dynamic melting. Experimentation set at an average HTF flow rate of 1 *l*/min and a PCM flow rate of 0.5 *l*/min.

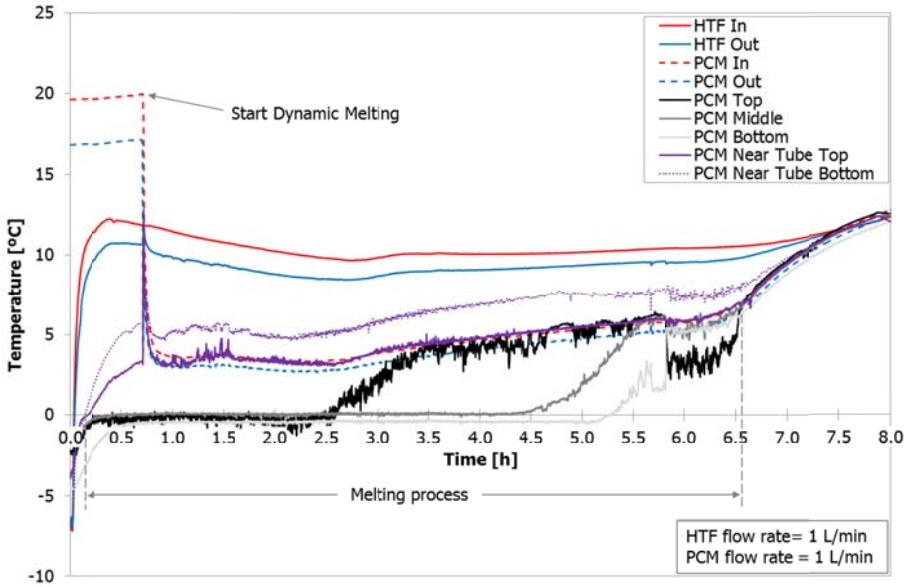

Fig. 5. Temperature evolution of the HTF and the PCM in a discharging process with dynamic melting. Experimentation set at an average HTF flow rate of 1 *l*/min and a PCM flow rate of 1 *l*/min.

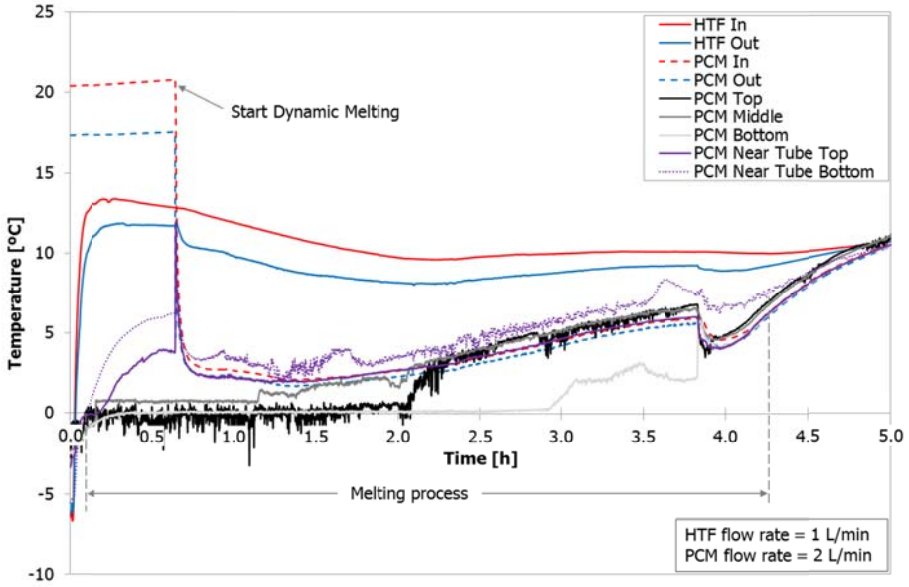

Fig. 6. Temperature evolution of the HTF and PCM in a discharging process with dynamic melting. Experimentation set at an average HTF flow rate of 1 *l*/min and a PCM flow rate of 2 *l*/min.

Fig. 7 shows the local effectiveness during the melting process with respect to the PCM liquid fraction for a HTF flow rate of 1 *l*/min with and without the influence of dynamic melting. It can be observed from Fig. 7 that during the baseline test, the effectiveness was initially high, reflecting the low resistance in heat transfer in the PCM. After this it decreased until the liquid fraction was 0.25, and remained constant until the liquid fraction was 0.4. From the liquid fraction of 0.4 to 0.75, natural convection is likely to have dominated maintaining the resistance relatively constant. Finally, at the end of the melting process, the effectiveness decreased due to

a loss of heat transfer area as the phase front decreased rapidly. The average effectiveness value during the baseline test was 0.088.

During the other processes all three effectiveness profiles before the beginning of the dynamic melting process were tracking below the baseline test profile. The differences were mainly due to slightly different boundary conditions and experimental errors. The three dynamic melting processes started at a liquid fraction of 0.095 ±0.005. Once dynamic melting was initiated, the effectiveness experienced a rapid decrease followed by a sharp increase. The sudden decrease was caused by the mixing of the PCM in the PCM recirculation loop which was at ambient temperature. Before the dynamic melting was activated, the liquid PCM was stratified both in the radial and axial directions: the liquid PCM located nearer the HTF tube was hotter than liquid PCM located nearer to the solid PCM, and the liquid PCM located at the top of the heat exchanger was hotter than liquid PCM located at the bottom. Therefore, when the PCM recirculation pump was switched on, the hotter liquid PCM located at the top and in the PCM recirculation loop passed through the entire outer wall of the HTF tube, causing the outlet HTF temperature to increase sharply and therefore a sharp decrease in the effectiveness. Very quickly, the liquid PCM was mixed due to the recirculation, which induced the temperature of the PCM to drop. As a consequence, the HTF outlet temperature sharply decreased, which caused a sharp increase of the effectiveness. When the liquid fraction was around 0.9, the effectiveness showed again a sudden increase. This is because a small block of ice remaining at the top of the tube would fall into the liquid PCM and cool the HTF. This small block was attached to the shell of the heat exchanger and as the PCM melted, the volume of the PCM reduced, leaving this block above the liquid level.

The magnitude of enhancement of the dynamic melting was related to the PCM flow rate. dynamic melting showed enhancement when the PCM flow rate was equal to or higher than the HTF flow rate, which is consistent with what was determined in Tay et al. [13]. The effectiveness was based on how close the HTF outlet temperature was to the PCM melting temperature. The PCM recirculation loop was adding heat into the PCM and the impact of this was to increase the HTF outlet temperature as it physically pumped warmer PCM in parallel to the tube and it increased the HTF outlet temperature, as observed in Table 1. Hence, it was found that the measured effectiveness was in fact an underestimated value since if the heat gains would have not existed the effectiveness would have been higher. The average effectiveness values during the melting process with PCM flow rates of 1 and 2 *l*/min were 0.109 and 0.137, respectively, which were 24.7% and 56.4% higher than the value obtained in the baseline test.

It was interesting to note that for the dynamic melting process at a PCM flow rate of 0.5 *l*/min, which turned to be lower than the HTF flow rate, there was a lack of improvement when compared to the baseline test. It was initially observed that when the dynamic melting process started, the effectiveness increased slightly. However, after this point the difference compared to the baseline test was small. Notice that if the heat gains did not occur in the PCM recirculation loop, then an improvement in effectiveness would have occurred at this PCM flow rate. At PCM flow rates of 1 and 2 *l*/min, which turned to be equal to or higher than the HTF flow rate, a significant increase in the effectiveness occurred for the liquid fraction range between 0.1 and 0.45. During this period, the resistance in the PCM was practically constant and much lower than that delivered by natural convection as occurred in the baseline test. The mixing due to the PCM recirculation was able to achieve these enhancements. For the liquid fraction range between 0.45 and 0.9, it decreased gradually as a result of a heat transfer area loss since the PCM front became more two-dimensional.

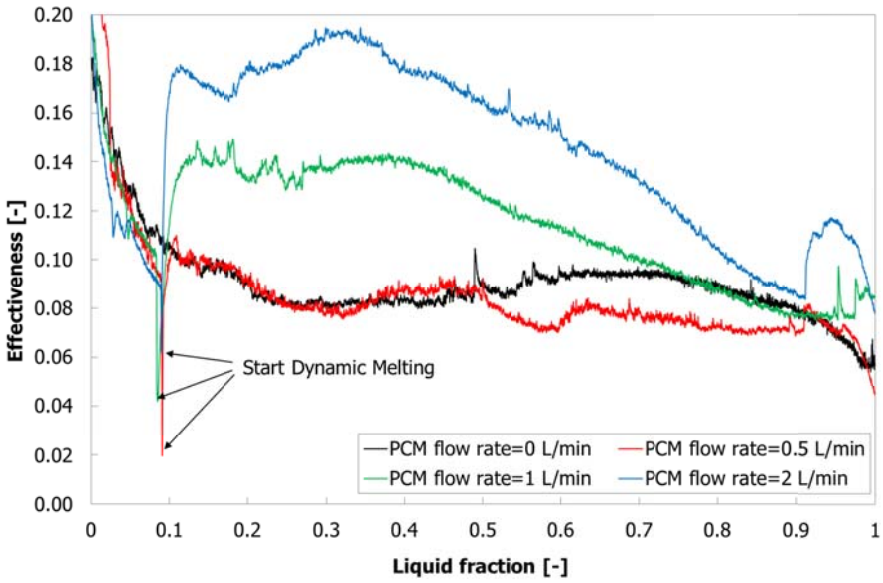

Fig. 7. Local effectiveness evolution during the melting process for an HTF flow rate of 1 *l*/min with and without the influence of the dynamic melting.

Fig. 8 shows the evolution of the energy released by the HTF, the heat gains in the PCM recirculation loop and the heat gains because of the boundary conditions during the phase change process. This evaluation allows studying the influence of the heat gains on the decreasing of the phase change process time and on the decreasing of the local effectiveness.

Notice that during the baseline test (Fig. 8a), basically all the energy absorbed by the PCM came from the HTF. At the end of the melting process, 92.7% of the energy removed from the PCM during the charging process was recovered, and only 7.3% was lost due to heat gains from

the surroundings. During the processes where the dynamic melting enhancement technique was implemented (from Fig. 8b to Fig. 8d), heat gains due to the recirculation of the liquid PCM outside the heat exchanger reduced the melting time. The energy absorbed by the PCM because of these heat gains was 32.6 ±0.9% of the energy stored during the charging processes, while the energy absorbed by the PCM from the surroundings represented the 3.5 ±0.3%. As a result of the heat gains, the PCM temperature was increased and therefore a reduction on the phase change period was obtained. Notice that the error from the energy balance of the experimentation carried out (Table 1) is less than the 11%, which shows that the results are validated.

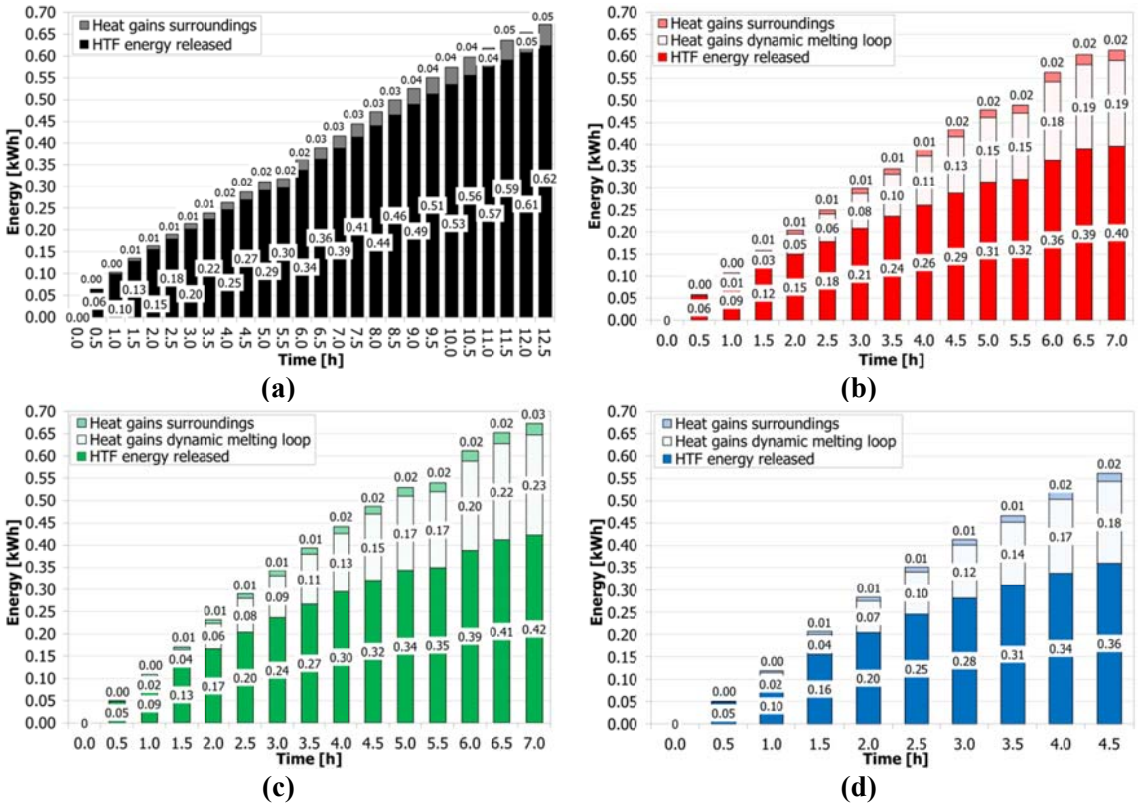

Fig. 8. Evolution of the energy absorbed by the HTF (straight full coloured bar), the heat gains because of the liquid PCM recirculation (white bar), and the heat gains because of the boundary conditions (dotted coloured bar) during the melting process for an HTF flow rate of 1 *l*/min. (a) Baseline test: PCM flow rate of 0 *l*/min; (b) dynamic melting: PCM flow rate of 0.5 *l*/min; (c) dynamic melting: PCM flow rate of 1 *l*/min; (d) dynamic melting: PCM flow rate of 2 *l*/min

Fig. 9 shows the change of the heat transfer rate of the HTF during the discharging process, with and without the influence of dynamic melting. Clearly, the impact of dynamic melting is to dramatically increase the heat transfer rate to the HTF. The average heat transfer value of the HTF during the baseline test was 49.1 W, while the average heat transfer value of the HTF during the dynamic melting for flow rates of 0.5, 1 and 2 *l*/min were 58.2 W, 62.1 W and 81.6

W, respectively. If compared to the baseline test, it represented an enhancement of 18.5, 26.3 and 66 %, respectively. Moreover, it was found that the heat transfer rates of the PCM recirculation loop were 32.9, 37.3 and 48.9 W, respectively. Therefore, if the heat gains were minimized, the heat transfer rate from the HTF would have been even higher, as the HTF would have been the only heat source melting the PCM. Furthermore, the influence of the pump in the PCM rate was found to be very small if compared to the average increase in the heat transfer rate from the dynamic melting. Values from the calculation showed that the heat introduced by the PCM recirculation pump during the dynamic melting for flow rates of 0.5, 1 and 2 *l*/min were $4.25 \cdot 10^{-5}$ W, $1.67 \cdot 10^{-5}$ W, and $1.09 \cdot 10^{-2}$ W, respectively.

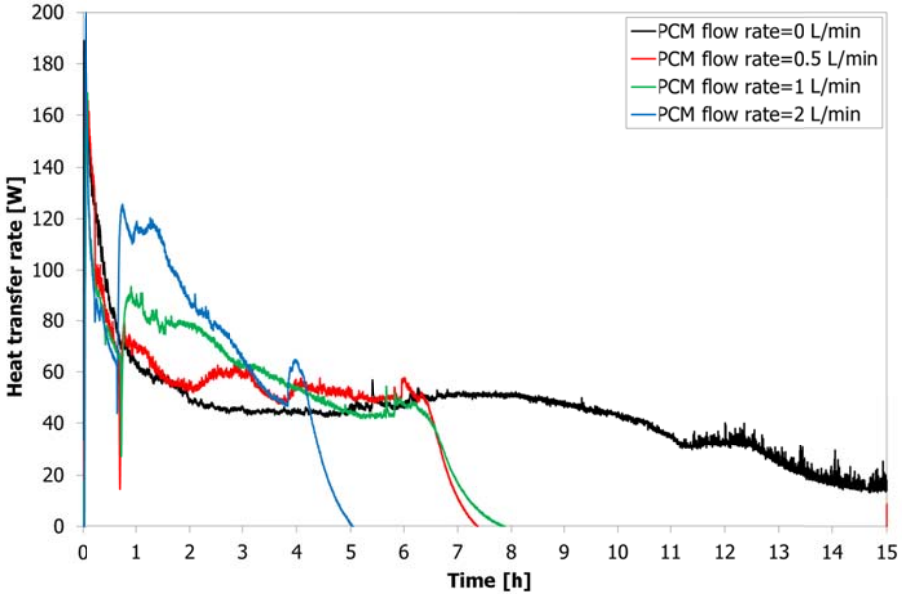

Fig. 9. Evolution of the HTF heat transfer rate during the discharging process for an HTF flow rate of 1 *l*/min with and without the influence of the dynamic melting.

Finally, Table 1 and Table 2 summarize the results obtained during the experiments and show the enhancements of the dynamic melting.

Table 1. Summary of the results obtained for the different experiments carried out.

PCM flow rate	**Melting process time**	**Dynamic melting process start**	**Average T.PCM.in**	**Average T.PCM.out**	**E_{HTF}**	**$E_{HG.BC}$**	**$E_{HG.loop}$**	**E_{PCM}**	**Average $\dot{Q}_{HTF}$**	**Average $\dot{Q}_{HG.BC}$**	**Average $\dot{Q}_{HG.loop}$**	**Average $\dot{Q}_{PCM}$**	**Average P_L**	**Average effectiveness**	**Energy balance error**
l/min]	[h]	[h]	[ºC]	[ºC]	[kWh]	[kWh]	[kWh]	[kWh]	[W]	[W]	[W]	[W]	[W]	[-]	[%]
Experimentation without dynamic melting															
0	12.3	-	-	-	0.62 (92.7%)	0.05 (7.3%)	-	0.67 (100%)	49.14	3.89	-	53.03	-	0.09	9
Experimentation with dynamic melting															
0.5	6.61	0.71	5.66	4.58	0.40 (64.5%)	0.02 (3.8%)	0.19 (31.7%)	0.61 (100%)	58.22	3.47	32.87	94.56	$4.25 \cdot 10^{-5}$	0.08	3
1	6.55	0.72	4.57	3.97	0.42 (62.7%)	0.03 (3.8%)	0.23 (33.5%)	0.68 (100%)	62.07	3.75	37.30	103.12	$6.80 \cdot 10^{-4}$	0.14	11
2	4.26	0.65	3.80	3.43	0.36 (64.0%)	0.02 (3.2%)	0.18 (32.8%)	0.56 (100%)	81.56	3.99	48.90	134.45	$1.09 \cdot 10^{-2}$	0.14	8

Table 2. Comparison of the dynamic melting enhancements.

PCM flow rate	**Change in melting process time**	**Average Q_{HTF}**	**Change in average effectiveness**
0	-	-	-
0.5	47.4 %	18.5 %	-4.5 %
1	47.8 %	26.3 %	24.7 %
2	65.3 %	66.0 %	56.4 %

4 Conclusions

A heat transfer enhancement technique known as dynamic melting (dynamic melting) has been experimentally tested in a cylindrical shell-and-tube heat exchanger using water as PCM. This enhancement technique consists of externally recirculating the liquid PCM during the melting process using an external pump, thereby increasing the overall heat transfer coefficient. Different experiments were carried out with a constant HTF flow rate of 1 *l*/min and varying PCM flow rates: 0, 0.5, 1 and 2 *l*/min. Only the parallel flow arrangement has been studied.

The experimental results showed that the phase change processes with the dynamic melting technique were 47.4%, 47.8% and 65.3% faster than the baseline test for flow rates of 0.5, 1 and 2 *l*/min, respectively. However, this enhancement was not only due to the increase in the overall heat transfer coefficient because of the forced convection, it was also due to the heat gains from the PCM recirculation loop. These heat gains increased the PCM temperature, and represented the 32.5 ±1% of the energy stored during the charging processes, which decreased the energy capacity of the LHTES unit. As for the effectiveness, the implementation of the dynamic melting technique only showed an enhancement when the PCM flow rate was equal or higher than the HTF flow rate due to the influence of the heat gains. During the dynamic melting processes with PCM flow rates of 1 and 2 *l*/min, the average effectiveness was respectively 24.7% and 56.4% higher than the effectiveness during the baseline test. In terms of heat transfer rates, dynamic melting represented an enhancement of 18.5%, 26.3% and 66% for flow rates of 0.5, 1 and 2 *l*/min, respectively. However, these heat gains are a characteristic of the experiments and not what can be expected in a real application. Hence, if the heat gains did not exist the effectiveness would be higher. An analysis of the pumping power associated with dynamic melting was shown to be negligible relative to the heat transfer improvements.

Acknowledgements

The authors acknowledge the South Australian Department of State Development who have funded this research through the Premier's Research Industry Fund - International Research Grant Program (IRGP 33). This project has received funding from the European Commission Seventh Framework Programme (FP/2007-2013) under Grant agreement Nº PIRSES-GA-2013-610692 (INNOSTORAGE) and from the European Union's Horizon 2020 research and innovation programme under grant agreement No 657466 (INPATH-TES). Jaume Gasia would like to thank the Departament d'Universitats, Recerca i Societat de la Informació de la Generalitat de Catalunya for his research fellowship (2016FI_B 00047). The work is partially

funded by the Spanish government (ENE2015-64117-C5-1-R). The authors at the University of Lleida would like to thank the Catalan Government for the quality accreditation given to their research group GREA (2014 SGR 123).

References

1. Zalba B, Marín José Ma, Cabeza LF, Mehling H. Review on thermal energy storage with phase change: materials, heat transfer analysis and applications. Applied Thermal Engineering 2003;23:251–83. doi:10.1016/s1359-4311(02)00192-8.
2. Cabeza L, Mehling H, Hiebler S, Ziegler F. Heat transfer enhancement in water when used as PCM in thermal energy storage. Applied Thermal Engineering 2002;22:1141–51. doi:10.1016/s1359-4311(02)00035-2.
3. Velraj R, Seeniraj R, Hafner B, Faber C, Schwarzer K. Experimental analysis and numerical modelling of inward solidification on a finned vertical tube for a latent heat storage unit. Solar Energy 1997;60:281–90. doi:10.1016/s0038-092x(96)00167-3.
4. Gil A, Oró E, Miró L, Peiró G, Ruiz Á, Salmerón JM, et al. Experimental analysis of hydroquinone used as phase change material (PCM) to be applied in solar cooling refrigeration. International Journal Of Refrigeration 2014;39:95–103. doi:10.1016/j.ijrefrig.2013.05.013.
5. Nithyanandam K, Pitchumani R. Analysis and optimization of a latent thermal energy storage system with embedded heat pipes. International Journal Of Heat and Mass Transfer 2011;54:4596–610. doi:10.1016/j.ijheatmasstransfer.2011.06.018.
6. Shabgard H, Bergman T, Sharifi N, Faghri A. High temperature latent heat thermal energy storage using heat pipes. International Journal Of Heat and Mass Transfer 2010;53:2979–88. doi:10.1016/j.ijheatmasstransfer.2010.03.035.
7. Sarı A, Karaipekli A. Thermal conductivity and latent heat thermal energy storage characteristics of paraffin/expanded graphite composite as phase change material. Applied Thermal Engineering 2007;27:1271–7. doi:10.1016/j.applthermaleng.2006.11.004.
8. Tong X, Khan JA, Ruhulamin M. Enhancement Of Heat Transfer By Inserting A Metal Matrix Into A Phase Change Material. Numerical Heat Transfer, Part A: Applications 1996;30:125–41. doi:10.1080/10407789608913832.
9. Khodadadi J, Fan L, Babaei H. Thermal conductivity enhancement of nanostructure-based colloidal suspensions utilized as phase change materials for thermal energy storage: A review. Renewable And Sustainable Energy Reviews 2013;24:418–44. doi:10.1016/j.rser.2013.03.031.

10. Zipf V, Neuhäuser A, Willert D, Nitz P, Gschwander S, Platzer W. High temperature latent heat storage with a screw heat exchanger: Design of prototype. Applied Energy 2013;109:462–9. doi:10.1016/j.apenergy.2012.11.044.
11. Pointner H, Steinmann W-D, Eck M. Introduction of the PCM Flux Concept for Latent Heat Storage. Energy Procedia 2014;57:643–52. doi:10.1016/j.egypro.2014.10.219.
12. Tay N, Bruno F, Belusko M. Experimental investigation of dynamic melting in a tube-in-tank PCM system. Applied Energy 2013;104:137–48. doi:10.1016/j.apenergy.2012.11.035.
13. Tay N, Belusko M, Liu M, Bruno F. Investigation of the effect of dynamic melting in a tube-in-tank PCM system using a CFD model. Applied Energy 2015;137:738–47. doi:10.1016/j.apenergy.2014.06.060.
14. Tay N, Belusko M, Bruno F. An effectiveness-NTU technique for characterising tube-in-tank phase change thermal energy storage systems. Applied Energy 2012;91:309–19. doi:10.1016/j.apenergy.2011.09.039.
15. López-Navarro A, Biosca-Taronger J, Torregrosa-Jaime B, Corberán J, Bote-García J, Payá J. Experimental investigations on the influence of ice floating in an internal melt ice-on-coil tank. Energy And Buildings 2013;57:20–5. doi:10.1016/j.enbuild.2012.10.040.
16. Akgün M, Aydın O, Kaygusuz K. Experimental study on melting/solidification characteristics of a paraffin as PCM. Energy Conversion And Management 2007;48:669–78. doi:10.1016/j.enconman.2006.05.014.